

VYSOKÉ UČENÍ TECHNICKÉ V BRNĚ  
FAKULTA STROJNÍHO INŽENÝRSTVÍ  
ÚSTAV MATEMATIKY

**Mgr. Michaela Honková**

**NUMERICAL METHODS OF IMAGE ANALYSIS  
IN ASTROMETRY**

NUMERICKÉ METODY ANALÝZY OBRAZU V ASTROMETRII

Zkrácená verze Ph.D. Thesis

Obor:	Aplikovaná matematika
Školitel:	Prof. RNDr. Miloslav Druckmüller, CSc.
Oponent:	Prof. Alan Fitzsimmons
Datum obhajoby:	9. května 2018

**Keywords**

astrometry, image processing, flatfield, filters

**Klíčová slova**

astrometrie, zpracování obrazu, flatfield, filtry

**Rukopis dizertační práce je uložen**

v Areálové knihovně Fakulty strojního inženýrství  
Vysokého učení technického v Brně.

# Contents

<b>1</b>	<b>Introduction</b>	<b>3</b>
<b>2</b>	<b>Astrometry of asteroids and comets</b>	<b>4</b>
2.1	Asteroids and comets . . . . .	4
2.2	Astrometry of NEOs . . . . .	4
2.2.1	Image acquisition . . . . .	5
2.2.2	Image pre-processing . . . . .	7
2.2.3	Image astrometry . . . . .	8
2.3	Kleť Observatory . . . . .	9
2.3.1	Hardware . . . . .	9
2.3.2	Software and workflow . . . . .	10
2.3.3	Limitations . . . . .	11
<b>3</b>	<b>Background flattening</b>	<b>12</b>
3.1	Chosen background flattening methods . . . . .	12
3.1.1	Median flatfield . . . . .	12
3.1.2	Kappa-sigma clipping flatfield . . . . .	13
3.1.3	SMin flatfield . . . . .	14
3.1.4	$\alpha$ -quantile flatfield . . . . .	14
3.1.5	Unsharp masking filter . . . . .	15
3.1.6	Savitzky–Golay filter . . . . .	16
3.2	Comparison of performance . . . . .	19
3.2.1	Object detection in Blink . . . . .	19
3.2.2	Object measurement in Astrometry . . . . .	24
3.3	Recommendations for use . . . . .	26
<b>4</b>	<b>First results: Interstellar body 1I/2017 U1 ‘Oumuamua</b>	<b>27</b>
<b>5</b>	<b>Conclusion</b>	<b>28</b>
	<b>Bibliography</b>	<b>29</b>
	<b>Curriculum Vitae</b>	<b>31</b>



# 1 Introduction

Asteroids and comets are small bodies of the Solar System, orbiting the Sun along its planets. Some of them come dangerously close to the Earth and even collide with our planet, occasionally causing mass extinction event. An ability to track and compute position of these so-called Near-Earth Objects (NEOs) ahead of time gives us unprecedented opportunity to avoid this natural hazard to mankind. The measuring of their positions on the sky in given time is called astrometry and briefly described in Section 2.2. The most critical task is obtaining enough of precise positional data of newly discovered objects, called follow-up astrometry, which is essential to compute meaningful orbit of the object.

Kleť Observatory, located on top of Kleť mountain in Blanský forest, operates the biggest telescope in Europe dedicated to follow-up astrometry of NEOs. Their digital images suffer from very uneven background, hindering the performance — or even the possibility — of astrometric measurement. Due to the problems described in Section 2.3.3, the usual image pre-processing methods cannot be used in the case of Kleť Observatory. Six newly designed filters are proposed in Section 3.1 to handle the needs of Kleť Observatory, programmed into software the author is developing, and tested on sample data. Their performance is compared in Section 3.2 and recommendations for their use by the observer are assembled. These filters allow for construction of artificial flatfield (background image), from as little as a single digital image, used to remove the uneven background, eliminating the need to take calibration images during the observation, and allowing re-measurement of vast image archives for which no calibration images are available.

The new filters were immediately put to use to allow astrometry of the first interstellar object 1I/2017 U1 (*'Oumuamua*), as described in Chapter 4. The work is closing with Conclusion in Chapter 5, being followed by the Bibliography, author's CV, and the abstract.

## 2 Astrometry of asteroids and comets

### 2.1 Asteroids and comets

Asteroids and comets are solid bodies of the Solar System orbiting the Sun together with planets and dwarf planets. Their sizes range from several meters to hundreds kilometers big boulders. There is an estimated amount of millions of these bodies in the inner Solar System alone. To be able to track these bodies, a set of *orbital elements* is computed for each.

There are many subcategories of asteroids and comets sorted by their orbit type. Of an immediate interest to mankind are NEOs, Near-Earth Objects. NEOs are asteroids and comets with *perihelion distance* less than 1.3 AU, placing them inside the inner Solar System. There are over 17 700 discovered NEOs as of January 2018 <sup>1</sup>.

About 8 000 of known NEOs have diameter over 140 meters, which makes them capable of causing local disaster upon impact, while about 900 known NEOs have diameter bigger than 1 kilometer, having the potential to cause mass extinction event upon impact to the Earth. To evaluate the risk and predict possible impacts, accurate orbits must be computed, which requires precise astrometry of asteroids and comets to be carried out.

### 2.2 Astrometry of NEOs

Astrometry is a precise measurement of positions and movements of celestial bodies. It includes observational techniques, instrumentation, processing and analysis of observational data, positions and motions of bodies and reference frames, and it relies on a number of theoretical aspects, which relate the observations to the laws of physics. Among the most important are celestial mechanics, optics, theory of space and time references, astrophysics, and statistical inference theory.

Astrometry allows for discovery and tracking of NEOs by detecting these faint, moving bodies against the background of catalogued stars. Especially for observatories focused on NEOs research, flexibility in observing plan is crucial. Smaller NEOs are often discovered when passing close to the Earth and failure in promptly obtaining enough data to determine their orbit results in inevitable loss of the object. Accordingly, newly discovered NEO should be observed and its astrometric positions sent to the Minor Planet Center (MPC) as soon as feasible. The astrometric observations of minor bodies are collected and processed by Minor Planet Center (MPC), which

---

<sup>1</sup><http://neo.jpl.nasa.gov/stats/>

operates at the Smithsonian Astrophysical Observatory, under International Astronomical Union. The MPC is responsible for the designation of minor bodies (asteroids, comets, moons) in the Solar System, for the efficient collection, computation, checking and dissemination of astrometric observations and orbits of minor planets and comets.

With the additional data available, the accuracy of the object's orbit increases and there is more time available to obtain further observations before the object would become lost due to its deviation from its predicted position. With enough observations, the computed orbit becomes precise enough to allow for recovering the body at its next favorable apparition. This fast and accurate astrometry of newly discovered bodies is called follow-up astrometry. Examples of its profound effect on body's orbital parameters accuracy can be found in my Bachelor's work [6].

The images entering astrometry are affected by various errors, translating into inaccuracy in obtained position. That leads to inaccuracy in computed orbit, and then of predictions of the body's positions (and possible impacts to the Earth) in future. As there are only a few observations available soon after the discovery, the accuracy of every single one is that more important. Their insufficient quality can result in loss of the object, thus follow-up astrometry has to be not only quick, but also precise. The essential requirements for sufficient astrometric precision are given by the 80 characters long format, in which the observations are sent to MPC<sup>2</sup> and are as follows:

- Time measured to accuracy under 1 second
- Topocentric position determined to at least 15 meters
- CCD image with small pixels, high dynamic range, low noise and high quantum efficiency
- Stellar catalog with high accuracy evenly covering the sky
- Image processing at least partially automatized
- Robust astrometric method

### 2.2.1 Image acquisition

Large reflector telescopes mounted in observatories' domes equipped with CCDs and manipulated by remotely controlled motors are the norm of today's professional observational astronomy. A CCD works using photoelectric effect. Its image chip consists of a matrix of capacitors covered with a layer of light-sensitive semiconductors which, upon absorbing photons, expel electrons. The electron charge accumulates in the capacitors and at the end of

---

<sup>2</sup>described at <http://www.minorplanetcenter.net/iau/info/OpticalObs.html>

exposition the total charge of electrons on each CCD pixel is amplified, converted to voltage and further to ADU (Analog Digital Units). CCDs have very high quantum efficiency, thus their resolution is limited mainly by seeing of the atmosphere, and are capable of recording the observation in a form of an image file for later, repeated use.

The images are typically taken by a CCD in grayscale, meaning every photon regardless of its wavelength (color) results in an electron gain as given by the camera's spectral sensitivity by its manufacturer, and the information of its color is therefore lost. Astronomical images use special file formats, which allow for appending various data about the conditions the image was taken in in the file's header and saving the image data without compression, which is crucial for subsequent scientific use.

The methodology for coordinate determination derived for photographic plates remained principally the same. The accuracy of measurements improved down to 1 mas (milliarcseconds), but the image processing became much quicker because of computers, which allowed for advanced and near-automatic image processing. Since the precision of astrometric measurements in modern time is so high, many small sources of inaccuracies[2] have to be dealt with, which were negligible in past. Going from the source to the detector and then to the final image, the quality of the final image may be affected by following

**Image distortions:**

- *cosmic rays*, which are high energy particles coming randomly from the space
- *scintillation*, an apparent flickering of position and brightness of the object, caused by the packets of light passing through the atmospheric cells with different refractive index
- *sky brightness*, diffused light which is present on the night sky even in absence of light sources of interest
- *Airy disc* due to light diffraction
- *aberrations*, caused by nonideal mirrors and lenses
- *vignetting*, which occurs when the arriving wavefront is truncated by objects in different planes obstructing the incoming light
- *dust particles*, which may be present on the chip
- *defect pixels* in a form of hot and cold pixels, as well as varying light sensitivity of pixels
- *bleeding* streaks around bright stars
- *photon noise* due to fluctuation of photons arriving during exposure time
- *thermal noise* caused by dark current on the CCD chip
- *Read-out noise* on the CCD chip's amplifier



Joining together all of these effects, the quality of the image can be expressed by SNR (Signal to Noise Ratio), which is the ratio of the useful obtained signal versus the total signal including all the noise.

### **2.2.2 Image pre-processing**

As NEOs pose moving targets, there may be very short window of opportunity for observations. The observations have to be done in less than ideal conditions, providing noisy images. In addition to the noises mentioned in previous paragraph, we may have to do with images containing a gradient from a nearby bright star or the Moon, dense stellar field of Milky Way, or NEO imaged close to a corner of the field of view. It is essential to pre-process the images before reducing them to objects, for which a handful of simple techniques are used.

Multiple shorter exposures can be stacked in various ways to reduce noise of the image. Calibration images can be taken and then applied on the data images. Only their basic explanation is stated in this part, please refer to the thesis for details.

#### **Bias Frames**

These are images taken with closed shutter of the CCD and shortest possible exposure time and serve to remove electrons related noise from the CCD image. Bias still contains read-out noise, therefore it is better to take more bias images and use their median.

#### **Dark Frames**

These are taken with closed shutter of the CCD and the same exposure, temperature and binning as the image we want to remove the noise from. They include bias and thermal noise of the CCD chip, but are affected by read-out noise, therefore its better to use median of several dark frames. An observatory can create a library of dark frames ahead. If the thermal noise is negligible, bias frames are used instead.

#### **Flatfields**

Flatfield is taken with CCD shutter open, at the target exposure time and against evenly lit background. It accounts for different pixel sensitivity, dust particles in the optical system and vignetting. Flatfields represent the response of the whole optical system. The pixel values are normalized to lay between 0 and 1 and the final image is then multiplied or divided by the flatfield. Dark frame should be applied to the flatfields as to any other image. Observatories often create libraries of master flatfields.

## Filtering

*Filtering* is generally not used by observatories performing astrometric measurements.

### 2.2.3 Image astrometry

The CCD images entering the astrometry typically have dark frame or bias and flatfield applied. Sometimes co-adding is used, but further image processing is not employed. Most of the average astrometry is done by one of the available programs capable of astrometric measurements, notably Astrometrica.at, or SAO Image. The details of their algorithms are not usually provided, thus truly dedicated observatories create their own astrometric software, typically in cooperation with their home universities. This serves two purposes: the observatory can adjust the software to their own specific needs, and the worldwide astrometric measurements avoid cumulating possible systematic errors.

Astrometric procedure determines the coordinates of the observed objects in comparison to the known stars on the image. Stellar catalogs are used for this purpose, therefore quality catalog is essential for high precision astrometry. Ideal star catalog should be 'dense and deep', offering stars of varying brightness distributed across entire sky, for astrometry to be carried out regardless of asteroid's brightness and position. UCAC4 catalog is the most precise astrometric catalog to date and recommended by Minor Planet Center for observers to employ.

Astrometry produces equatorial coordinates of the measured object in the time of observation. These are sent to Minor Planet Center with precision 0.01 second in right ascension and 0.1 arcsecond in declination, unless higher precision is warranted. To keep the quality of the included data high, MPC compares the astrometric measurements with the expected positions and inconsistent measurements are rejected by their automatic system. Astrometric measurements should consistently have an error lower than 1" for observations using the same comparison stars.

Automated astrometry is so far the unreachable dream in the field. The automated astrometry in general either lacks completeness (does not recognize part of the objects present on the images) or it lacks reliability (generates a lot of false detections). The human brain is still unmatched in its ability to recognize faint targets on images and skilled observer is the choice of the observatories.

## 2.3 Klet' Observatory

Klet' Observatory is located 1068 meters above sea level in southwestern part of the Czech Republic in a protected landscape area with Bortle's dark sky class 1 to 2. Typical seeing on the site is 1.5–2". The observatory ranks among the worlds most prolific professional NEO follow-up programmes. Klet' Observatory's team consists currently of just two members, but handles the largest telescope in continental Europe used exclusively for astrometric observation of asteroids and comets. The program includes confirmation of newly discovered NEO candidates, early follow-up of newly discovered NEOs, long-arc follow-up of NEOs in need of further astrometric data, recovery of lost NEOs and detection of cometary features. The highest priority is given to Virtual Impactors and Potentially Hazardous Asteroids.

Klet' Observatory has been carrying out astrometric measurements since 1969 using photographic plates, and since 1994 using CCD. Starting in 2002, it operates 1.06-m KLENOT telescope, the largest telescope in Europe used exclusively for follow-up astrometry of asteroids and comets. Klet' Observatory developed a workflow allowing for astrometric positions to be sent within few minutes of images' acquisition. The KLENOT project contributed 52 658 astrometric measurements of 5 867 bodies to Minor Planet Center between 2002 and 2008. Since 2014, KLENOT project cooperates with Space System Awareness Program of European Space Agency and obtained total 27 426 astrometric measurements of 3 455 bodies between October 2014 and February 2017.

### 2.3.1 Hardware

Klet' Observatory uses two reflectors, 1.06-m KLENOT telescope and 0.57-m telescope, both equipped with CCDs. Only data from the KLENOT telescope are dealt with in the thesis. The 1.06-m KLENOT telescope is equipped with computer controlled parallactic mount. Calibration images are not used. The whole setup, meaning the camera, mount and the dome, is operated from a control room.

#### KLENOT Telescope

1.06-m f/3 main mirror + 4-lenses primary focus corrector

f/2.7 optical system

CCD camera FLI ProLine PL-230, thermoelectric cooling (since 2013)

chip e2v 2048x2048 pix, pixel size 15 microns, scale 1.1''/pix

FOV 37'x37', limiting magnitude 22 mag for 120s exposure time

### 2.3.2 Software and workflow

The observing process can be divided into several steps, each of which has its own software developed directly by Kleť Observatory to keep control over all of the aspects of the processing and of future development. The observing time is taken from freeware program *AboutTime*, which provides the CCD-controlling computer with averaged time, including correction from chosen servers, to a subsecond precision.

The *Ephem* tool lists the observable objects of desired category and brightness in right ascension order. Observational priority is given to NEOCPs<sup>3</sup>, V.I.s<sup>4</sup>, minor bodies scheduled for observation by radio telescopes, and NEOs with high orbit uncertainty [1].

A set of the target object's images is taken and its up to the observer, supplemented with custom tool *Blink*, to identify the object. *Blink* is developed by the author of this work and can adjust the contrast, smooth the images, and automatically align them. *Blink* can animate the images of the set, making it easier for the observer to spot moving object, and stack the images to effectively lengthen their exposure time and therefore raise SNR, and even stack images on a moving target. The last technique was immediately used to obtain astrometry of dwarf planet (136472) Makemake[3]. In addition, KLENOT team developed an algorithm to mark spots where known asteroids and comets are expected on the image, which was also implemented into *Blink* to further simplify the work of the observer.

The *Astrometry* tool is used to reduce the image to objects and carry out the astrometry utilizing a stellar catalog. Although the core of *Astrometry* was written in 1993, new astrometric catalogs are implemented when available and the software is being continually upgraded. The identification of stars is carried out employing similarity of triangles. The newest UCAC4 stellar catalog is used for identification of stars[15]. Plate parameters are computed, stars' positional errors are determined and standard 80 character output is produced for the targeted object. Typical SNR of observed targets, as measured by the program, is around 5, though it can be as low as 0.1 or as high as 20. The measured data is also automatically added to local MySQL databases.

The *Residua* tool is ran and the observed positions of the object are compared with ephemerides computed using local orbital elements database, which is updated daily with new Minor Planet Center data. The observer can therefore

---

<sup>3</sup>NEO Confirmation Page of Minor Planet Center with newly discovered asteroids in acute need of confirmatory observations

<sup>4</sup>Virtual Impactors, asteroids with nonzero collision probability within the next 100 years

verify the correctness of the identification and possibly drop the observations with higher error before sending them to Minor Planet Center. The whole process from taking the image set to sending out the object’s observations takes up to several minutes.

The usual astrometric accuracy of professional observatories is under 0.5–0.7”, depending on the star catalog used. The Kleť Observatory’s average astrometric error for KLENOT telescope was  $0.05 \pm 0.44$  in RA and  $-0.03 \pm 0.45$  in Dec between 2013 and 2017.

### 2.3.3 Limitations

The algorithm of *Astrometry* described in the thesis performs very well on an image taken by KLENOT telescope in ideal conditions, requiring dark, moonless nights with low humidity, the measured object not being close to the edges of the CCD and without bright stars being in the field of view, and shorter exposure times being used. However, such ideal conditions are often not possible.

As Kleť Observatory does not use calibration images, the background is very uneven due to many contributing factors, including fringing, vignetting, and background gradient from various sources, and also other random noise, to the point of being unable to carry out astrometric measurements at all. Additionally, starting to use calibration images as of now (2018) helps very little with mining information from the vast archive of Kleť Observatory, containing over 150 000 digital images.

The weak point of the astrometric process is assuming level background on the image. SNR threshold set by the observer is used to reduce the image to objects, their position refined by fitting through a Gaussian profile. Whenever the strict assumption of level background is not locally satisfied, the astrometry is burdened by error. Even worse situation occurs for objects in darker parts of the image, where the intensity values are under the global average background computed by the program, making the object literally undetectable by *Astrometry* even when the observer can see it. On the other end of the problem are brighter parts of the image, where even random noise is bright enough to be confused for objects by *Astrometry* program. Constructing an artificial flatfield to level the background of the images will have an undisputable impact on astrometry of KLENOT project.

## 3 Background flattening

### 3.1 Chosen background flattening methods

Since the KLENOT project observes very faint objects, usually only several pixels across in size, tampering with high frequency noise on the image will inevitably lead to corruption of the astrometric data. On the other hand, the low frequency noise (background) could be removed.

While many image processing methods are known, most are not suitable for our special case. These methods were carefully considered and the most promising ones were chosen. Some were adjusted to be suitable for our use as appropriate, and new methods were developed to deal with our images.

Six methods were developed for this work, where the first three deal with a set of consecutively taken images, which is the usual way of taking images for astrometric purpose, while the last three deal with a single image. They were programmed into *Blink*, software for image processing and viewing which the author of the thesis is developing for Klet' Observatory's needs, and tested for performance. *Blink* is routinely used for astrometric observations by Klet' Observatory, and newly carries out the new flatfield processes automatically when the user chooses the desired method.

#### 3.1.1 Median flatfield

Median filter is commonly used to reduce gaussian noise in the image, for which the images have to be precisely aligned with each other. Such use of median does not achieve background removal through artificial flatfield creation. However, photographers use median to remove moving objects from an image to take scenery photos at frequented places without the walking people being present on the resulting image. The median of values on each pixel of the set of images is used for the result, therefore a person walking across photographed scene present only in less than half of the images on given pixels is removed as the result.

The KLENOT telescope takes a set of images of each observed field of view. Its imperfect tracking causes the stars to 'walk' across the field of view, which led me to the idea of using median to create an artificial flatfield from the image set.

The images have to be normalized due to each image of the set having slightly different background. For each image of the set  $I_i(x, y)$ , where  $i = (1, \dots, N)$ , *Background* values  $\beta_i$  are computed according to *Astrometry* algorithm de-

scribed in the thesis. The images are normalized by

$$F_i(x, y) = \frac{\beta_i}{I_i(x, y)}. \quad (3.1)$$

This effectively turns the images into 'flatfields', although still containing stars and other objects. For each pair of  $(x, y)$ , The  $N$  values of  $F_i(x, y)$  are arranged from smallest to greatest into a sorted list

$$F_{(1)}(x, y) \leq F_{(2)}(x, y) \leq \dots \leq F_{(N)}(x, y),$$

and their *median*  $\tilde{F}(x, y)$  is the middle number of this sorted list,

$$\tilde{F}(x, y) = \begin{cases} F_{(\frac{N+1}{2})}(x, y) & N \text{ is odd} \\ \frac{1}{2}(F_{(\frac{N}{2})}(x, y) + F_{(\frac{N}{2}+1)}(x, y)) & N \text{ is even.} \end{cases}$$

In our case, median is computed  $x \cdot y$  times, once for each pixel  $[x, y]$  of the flatfields  $F_i(x, y)$  and the  $x \cdot y$  medians construct the resulting flatfield  $\tilde{F}(x, y)$ , which is applied back on the image set as usual.

### 3.1.2 Kappa-sigma clipping flatfield

Kappa-sigma clipping is an elaborate version of median filter from previous section, employing mean and iterative process to get around the most profound weaknesses of median filter. The filter was programmed into *Blink*. As with the median filter, it was not used to stack an image set, but to construct an artificial flatfield.

We will use the normalized images  $F_i(x, y)$  and their median image  $\tilde{F}(x, y) = e_k(x, y)$  from the previous section. Denoting  $J_1 = \{1, \dots, N\}$ , where  $N$  is the number of images in the set, and setting the iteration count  $k = 1$  for the first iteration, we calculate the standard deviation  $\sigma_k(x, y)$  of the pixel values around the median  $e_k(x, y)$ ,

$$\sigma_k(x, y) = \sqrt{\frac{1}{N} \sum_{i=J_k} (F_i(x, y) - e_k(x, y))^2}.$$

The values with deviations  $\kappa = 2$  relative to the standard deviation are excluded

$$J_{k+1}(x, y) = \{i \in J_k \mid |F_i(x, y) - e_k(x, y)| \leq \kappa \sigma\}$$

and the remaining values are averaged using arithmetic mean

$$e_{k+1}(x, y) = \frac{1}{|J_{k+1}|} \sum_{i=J_{k+1}} F_i(x, y).$$

Second iteration  $k = 2$  is ran to compute anew the standard deviation  $\sigma_k(x, y)$  and so on, repeating the process until there is no change in the arithmetic mean on 4th decimal place or 5 iterations are done. The arithmetic mean  $e_{k+1}(x, y) = D(x, y)$  then becomes the final value for the examined pixel  $[x, y]$ . The process is repeated for each pixel of the image.

The flatfield  $D(x, y)$ , comprised of the iterated means, is then applied on the image set as usual.

### 3.1.3 SMin flatfield

The previous two methods tend to leave 'shadows' of the brightest stars in the flatfield data. A possible solution is to construct the flatfield not from a median or its variations, but take the minimal values instead. This filter creates an image from minimal values on each pixel in the image set, which is method sometimes used to achieve defringing of the images. The correction image created by SMin filter has included noise equivalent to one image of the series. The method was adapted into *Blink* as follows.

As with Median flatfield in Section 3.1.1, the images of the set  $I_i(x, y)$ , where  $i = (1, .., N)$ , have to be normalized into  $F_i(x, y)$ . *Background* values  $\beta_i$  are computed according to algorithm of *Astrometry*, which can be found in the thesis, and the image is normalized using Equation 3.1.

Again, this effectively turns the images into 'flatfields' containing stars. The final flatfield is created from maximal values on each pixel  $(x, y)$  of the  $F_i(x, y)$  set, corresponding to the minimal values of  $I_i(x, y)$ , by equation

$$D(x, y) = \max_{\forall i} F_i(x, y).$$

The flatfield  $D(x, y)$  is applied back on the image set as usual.

### 3.1.4 $\alpha$ -quantile flatfield

This is a filter the author came up with to create an artificial flatfield for any single CCD image of mostly stellar field. It is not needed to work a set of images or take any calibration images. Originally, the intent was to improve background estimate for *Astrometry* program, by working with local background value instead of global background value. We could compute background in a given window, and stack these windows beside each other to create an image representation of the computed backgrounds, which in turn could be used as an artificial flatfield. The smaller the background windows, the finer details it can preserve, but the more affected by the stars it becomes.



There is also going to be intensity jumps at the edges between the windows. All this can be resolved by designing a filter instead, and computing background value for each pixel from a handful of its neighbors.

Let  $I(x, y)$  be a CCD image with measured intensities. The filter's mask the size of  $m \times m$ , where  $m$  is odd, is centered on a pixel  $I(x, y)$  and determines the part of image from  $I(x - \frac{m-1}{2}, y - \frac{m-1}{2})$  to  $I(x + \frac{m-1}{2}, y + \frac{m-1}{2})$  containing  $N = m \cdot m$  image pixels. These are arranged from smallest to greatest into a sorted list  $I_{(n)}$ , where  $n = (1, 2, \dots, N)$ ,

$$I_{(1)} \leq I_{(2)} \leq \dots \leq I_{(N)}.$$

The  $\alpha$ -quantile  $\tilde{I}(x, y)$  lies between 0 and 1 and is defined as such a value, that  $\alpha \cdot 100$  percent values in the sorted list  $I_{(n)}$  falls under  $\tilde{I}(x, y)$ . It is determined as

$$\tilde{I}(x, y) = I_{(\alpha(N+1))},$$

or its closest index. For  $\alpha = 0.5$ , the  $\tilde{I}(x, y)$  is median, for  $\alpha = 0.25$ , the  $\tilde{I}(x, y)$  is first quartile. The user chooses  $\alpha$ , for a stellar field it should be suitable to set  $\alpha \in (0.25, 0.5)$ .

The computation is carried out for all pixels  $(x, y)$ , and the resulting  $\alpha$ -quantile intensities  $\tilde{I}(x, y)$  form an artificial background image, which is then turned into flatfield by Equation 3.1 and applied on the original image  $I(x, y)$ .

The second controllable parameter of this method is the size of the filter  $m \times m$ . It should be big enough for the stars to constitute less than half (in case of median when  $\alpha=0.5$ ) of the filter's pixels, but not too large, since smaller background variations will get omitted with too big a mask.

The method was programmed into *Blink* and various  $\alpha$  and  $m$  were tested for performance.

### 3.1.5 Unsharp masking filter

This image sharpening technique is commonly used in astronomy to bring out the details in the image. Unsharp masking was programmed into *Blink*. The process consists of baseline or continuum estimation and subsequent subtraction.

Let's have a CCD image  $I(x, y)$ . First, heavy blur using a low-pass filter is applied to  $I(x, y)$ , resulting into  $I_B(x, y)$ . The blurred image is subtracted from the CCD image, creating a mask of edges and other high frequency

components of the image. This mask is then added to the CCD image.

$$J(x, y) = I(x, y) + \alpha(I(x, y) - I_B(x, y))$$

Scaling factor  $\alpha$  controls the strength of the unsharp masking effect. The degree to which  $I_B(x, y)$  is blurred controls what size structures the mask functions on most effectively: strongly blurred image enhances large structures but will miss small structures, while small subtle blurs enhance tiny structures but miss larger structures.

The low-pass filters chosen were Gaussian Blur (kernel  $7 \times 7$ ) and Box Blur (kernel  $7 \times 7$ ), since Gaussian kernel converges to Box kernel after a few passes. The filter strength parameter  $\alpha$  was set to  $\alpha = 1$ .

### 3.1.6 Savitzky–Golay filter

This filter, called *Savitzky–Golay*[10], but also *least squares*[8] or *DISPO* (Digital Smoothing Polynomials)[14], is widely used to smooth the data in analytical chemistry. Even though it has an exceptional features, it is rarely used in image processing. Savitzky–Golay filter works with only one image. The smoothing increases SNR without greatly distorting the signal.

The filter locally fits a low degree polynomial through a subset of the data by linear least squares method, one data point at time: each data point is replaced with a new value obtained from a polynomial fit to  $2n + 1$  neighboring points (including the point to be smoothed), with  $n \geq$  than the order of the polynomial. In general case, this would be achieved by using NURBS (NonUniform Rational B-Spline) fitting, which would be computationally burdensome with over 16 million pixels of our CCD images.

Savitzky–Golay filter derives from a particular formulation of the data smoothing problem. When the data points are equally spaced, which holds true for a CCD image, an analytical solution to the least squares equations can be found[7] in a form of a set of *convolution coefficients*, which enormously simplifies its application. The analytical solution is derived in the thesis. The convolution coefficients can be computed ahead of time and then applied on the data in a form of a *weighted moving average* filter, where the weights are the precomputed convolution coefficients.

*Moving average filter* is a special case of Savitzky–Golay filter, where the data is fitted with a straight line. If the underlying function is constant, or linearly changing (increasing or decreasing), then no bias is introduced into the result. Higher points on one end of the averaging interval are balanced

by lower points on the other end in the resulting average. However, if the underlying function has nonzero second derivative, a bias is introduced.

The idea of Savitzky–Golay filtering is to find filter coefficients  $c_n$ , that approximate the underlying function not by a constant (whose estimate is the average), but by a polynomial of higher order. Since the process of least squares fitting involves only a linear matrix inversion, the coefficients of a fitted polynomial are themselves linear in the values of the data. That means we can do all the fitting in advance for a given polynomial degree and window size, using a fictional data consisting of all zeros except for a single 1, and then do all the fitting with real data just by taking linear combinations of the result. That is the key advantage of Savitzky–Golay filter: there exists a particular set of filter coefficients  $c_n$  for which *weighted average* ‘automatically’ accomplishes the process of least squares fitting inside a moving window.

The method was popularized by Savitzky and Golay in [10], where they published tables of the convolution coefficients<sup>5</sup>, and was later extended for the treatment of 2D and 3D data. The filter got into widespread use after being included in [9].

The specific nature of Savitzky–Golay filter assumes that the underlying function can be locally well-fitted by a polynomial. When that is true, as for smooth line profiles not too much narrower than the filter window, Savitzky–Golay filtering is very useful. While the polynomial itself performs smoothing on the dataset, the 1st (and 3rd) derivative locates maxima and minima in the data, the 2nd derivative can be used for baseline flattening, and 2nd or 4th derivative can enhance the resolution of the data. The numerical derivatives are obtained by differentiating the fitted polynomial, which means that the derivatives are calculated for the smoothed data curve.

## Extrapolation into 2D

Savitzky–Golay filter can be extended for use on two-dimensional datasets, such as intensity values in a CCD image, which is composed of a rectangular set of pixels. The trick is to transform the rectangular grid into a single row by ordering the indices of the data points. Where the one-dimensional filter coefficients are found by fitting a polynomial in variable  $z$  to a set of  $m$  data points, the two-dimensional filter coefficients are found by fitting a polynomial in variables  $v, w$  to a set of  $m \times n$  data points. The process parallels the 1D-fitting, described in the thesis or found in [9].

---

<sup>5</sup>Some errors of the original paper are corrected in [11]

Let's choose a bi-cubic polynomial, with moving window  $m \times n$  having  $m = 7$ ,  $n = 5$ ,  $v = (-3, -2, \dots, 2, 3)$ ,  $w = (-2, -1, \dots, 1, 2)$  and the fitted polynomial is  $g = a_{00} + a_{10}v + a_{01}w + a_{20}v^2 + a_{11}vw + a_{02}w^2 + a_{30}v^3 + a_{21}v^2w + a_{12}vw^2 + a_{03}w^3$ . There are  $m \times n = 35$  data points in the moving window, indexed  $d_1, \dots, d_{35}$ ,

w \ v	-3	-2	-1	0	1	2	3
-2	d <sub>1</sub>	d <sub>2</sub>	d <sub>3</sub>	...			d <sub>7</sub>
-1	d <sub>8</sub>	d <sub>9</sub>	d <sub>10</sub>	...			d <sub>14</sub>
0				...			
1				...			
2	d <sub>29</sub>	d <sub>30</sub>	d <sub>31</sub>	...			d <sub>35</sub>

which become vector  $\mathbf{d} = (d_1 \dots d_{35})^\top$ . The Jacobian has 10 columns, one for each of  $a_{00}$  to  $a_{03}$ , and 35 rows, one for each pair of  $w$  and  $v$  values. Each row has the form,

$$J_{row} = 1 \quad v \quad w \quad v^2 \quad vw \quad w^2 \quad v^3 \quad v^2w \quad vw^2 \quad w^3.$$

The convolution coefficients are calculated as

$$\mathbf{C} = (\mathbf{J}^\top \mathbf{J})^{-1} \mathbf{J}^\top$$

The first row of  $\mathbf{C}$  contains 35 convolution coefficients, which are multiplied with the 35 data values, respectively, to obtain the polynomial coefficient  $a_{00}$ , which is the smoothed value. The convolution coefficients are applied by

$$g = \sum_{i=0}^p \sum_{j=0}^q a_{i,j} v^i w^j,$$

where  $p < m$  and  $q < n$ , proposed in [13].

## Application

Savitzky–Golay filtering for two-dimensional dataset was programmed into *Blink*. Two-dimensional convolution coefficients computed by Chandra Shekhar in [12] were used. Possible practical application of this filter for Klet' Observatory's needs include image smoothing to raise SNR, use of 2nd derivative of the filter for baseline flattening to remove background irregularities, and use of 4th derivative for resolution enhancement in case the observed asteroid happens to be too close to a nearby star to resolve the two apart. The last implementation, although appealing in case of dense stellar fields in the region of milky way on the sky, goes beyond the scope of this work and will not be carried out for now.

Upon choosing the Savitzky–Golay filter in the menu of *Blink*, the user can specify the filter parameters within boundaries of the included coefficient table: fitted polynomial degree  $M$ , the size of square filter window  $m \times m$  and the order of the derivative. The algorithm finds the corresponding  $m \times m$  filter coefficients,  $a_{00}$  for smoothing or  $a_{20}$  and  $a_{02}$  for the second derivative, in included file and applies the filter on the image by equation

$$g(x, y) = \sum_{i=-n_L}^{n_R} \sum_{j=-n_L}^{n_R} C_{(i,j)} f_{(x+i, y+j)},$$

for each  $(x, y)$  of the image excluding the  $n_L = n_R$  edges to compute the result. For smoothing (0th derivative), the  $C = a_{00}$ , and for 2nd derivative, partial derivative with respect to  $x$  is applied by setting  $C = 2a_{20}$ , then partial derivative with respect to  $y$  is applied on the result by setting  $C = 2a_{02}$ . Since the second derivative flattens the baseline, an extra intensity buffer has to be added to avoid the intensity values oscillating around zero.

## 3.2 Comparison of performance

The six methods detailed in previous chapter were programmed into *Blink*, an image processing and viewing software routinely used by Kleť Observatory, which the author of this work is developing. Image set of a typical stellar field was processed by these methods and the results were compared at first by human eye in *Blink*, as the observations rely on experienced human observer to identify the observed body, and then in Kleť Observatory’s astrometric program *Astrometry*, where the astrometric measurement of the objects are carried out.

### 3.2.1 Object detection in Blink

The images were taken by 1.06-m KLENOT telescope equipped with CCD camera on 8th June 2014. The set contains 13 images. On the Figure 1 we can see section of the the raw image 3 of the set on the top and corresponding sections of the corrected images under it in the order the six methods are described. The settings for *Background* and *Range*, which recomputes the images from the 65 536 intensities recorded by the camera to 256 intensities intended to be viewed by human eye, were kept the same between the processed images for clarity of comparison.

## Median flatfield

The flatfield was created as a median of the set, as described in Section 3.1.1, and applied back on the images. We can see dramatic increase in the image's quality on Figure 1, however the stars cast shadows on the corrected image. That is caused by the stars walking too slowly (or alternatively, the image set being too short) in the set of images used for the flatfield's creation.

## Kappa-sigma clipping flatfield

The flatfield was created by kappa-sigma clipping method described in Section 3.1.2 from the image set, removing outliers of standard deviation  $> 2$ , with maximum 5 iterations allowed, and the resulting flatfield was applied back on the images. On the Figure 1 we can see dramatic increase in the image's quality very similar to using median filter, but the stars cast slightly less pronounced shadows on the corrected image than they did with an image corrected by median filter.

## SMIN flatfield

The flatfield was created using SMIN method from the image set as per Section 3.1.3 and applied back on the images. In the Figure 1, we can see the stars no longer cast visible shadows on the result. Images treated with SMIN filter retain slightly more gaussian noise. The corrected image is slightly lighter because the minimal intensity chosen to represent a pixel is used as a denominator while creating a flatfield, resulting in lighter image. Usually, the image's contrast would be recomputed for human eye, which was omitted for the sake of more clear comparison between the methods.

## $\alpha$ -quantile flatfield

The flatfield was created from a single image using the new method described in Section 3.1.4, and applied back on the image. The processed image offers very sharp, even scene, however slight remnants of the background noise can be seen. The stars do not cast any shadow, but brighter stars developed a dark center. As these are too overexposed to be used in final astrometry computation anyway, this effect can be safely disregarded.

The filter's performance is controlled by two parameters, size of the filter  $m \times m$ , and  $\alpha$ , which specifies the quantile of the result. For the usual stellar field image, the best performance from the observer's point of view are reached for  $\alpha = 0.5$ , which is median, and  $m = 13$ .

## Unsharp masking filter

Unsharp masking method as described in Section 3.1.5 was applied on the image. The method works directly with an image without an assistance of flatfield creation. Strength of the filtering is controlled by scaling factor  $\alpha$  and the size of affected structures is controlled by the degree of blurring. There could be two possible ways for us to use this filter, which were tested.

**1) Heavy blur:** A very heavy blur in the first step should make stars disappear, which basically creates an approximate background image, which could be then used to create flatfield instead of carrying out the rest of the unsharp masking procedure. Since the image is blurred, small sized features will not be affected by the image processing.

It shows that not even heavy blur removes the stars due to the CCDs high dynamic range resulting in high difference between the background and the peaks of the stars. In astrophotography, stars would often be removed by hand, which is unacceptable for our purposes.

**2) Small filter kernel:** Unsharp masking filter with small kernel blur should affect small structures on the image, effectively enhancing their contrast and thus raising SNR, making the faint asteroids easier to measure.

While the processed image itself may look sharper to human eye overall, closer inspection reveals that it is substantially noisier. The filter enhanced contrast in noise just as well as in the real features. It is a common misuse of this very popular and widely used filter to try to bring faint objects out of the sky's background. When trying to enhance faint features like asteroids and faint stars out of the background, we are just as likely to elevate local noise to the status of star-hood. Images suitable for this filter should have high SNR and low contrast scenes with fine details we wish to enhance, which is the direct opposite of our images. For low SNR and high contrast stellar field, this method is highly unsuitable. This illustrates that a popular, widely used method which is recommended often does not guarantee good results. Understanding of the mathematics behind the filter's method is essential to picking correct filter.

## Savitzky–Golay filter

This filter works directly on single image without an assistance of flatfield creation. User chooses the fitted polynomial degree  $M$  and the size of square filter window  $m \times m$ . *Blink* finds the corresponding  $m \times m$  filter coefficients in included file and applies the filter on the image.

The 2nd derivative of Savitzky–Golay filter easily removes the background, but has adverse effect on stellar objects which would interfere with astrometric measurements.

## Recapitulation

The adjusted images are set side by side for better comparison on Figure 1. The first three filters work with an image set and offer good background removal, although SMIN filter seems the best.  $\alpha$ -quantile filter is slightly worse, but can be used with a single image. Unsharp masking filter only adds more noise, and Savitzky–Golay filter evens the background sacrificing the ability to perform the astrometric measurement altogether.



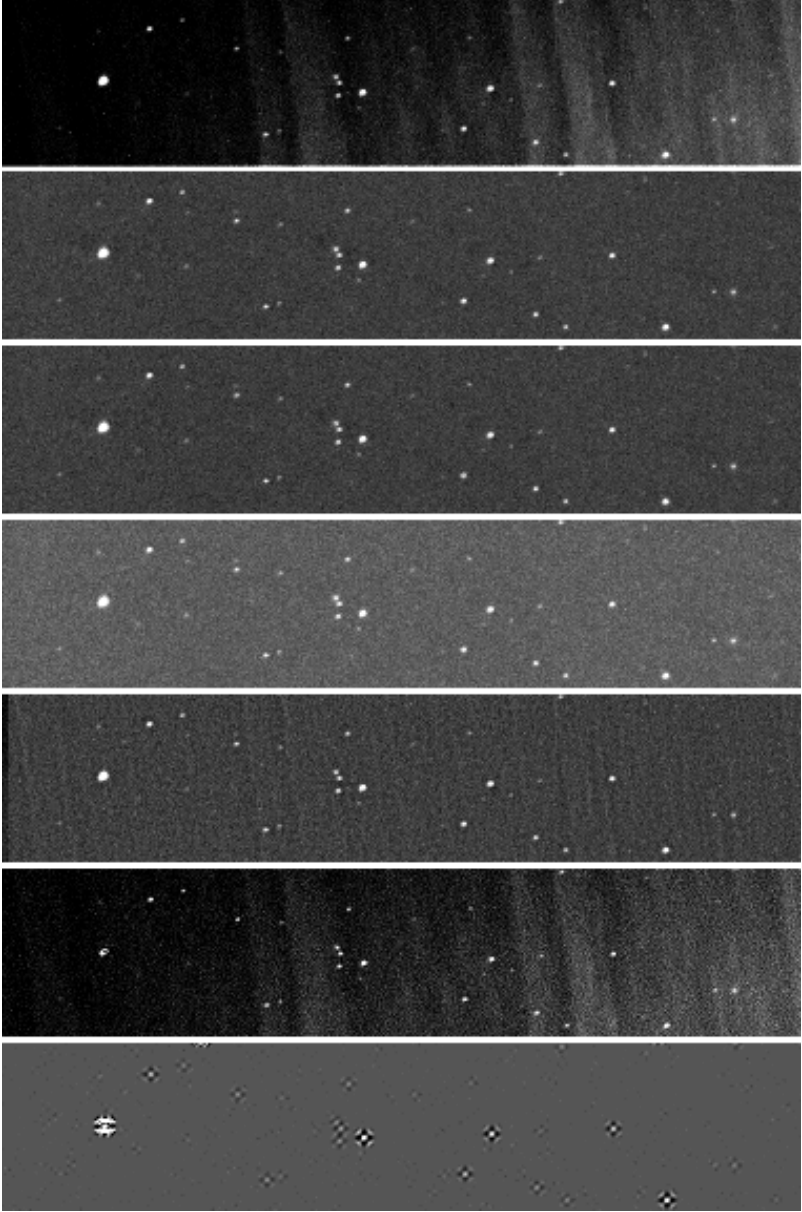


Figure 1: Comparison, from top to bottom: Raw image, Median flatfield, Kappa-sigma clipping flatfield, SMIN flatfield,  $\alpha$ -quantile flatfield ( $\alpha = 0.5$ ,  $m = 13$ ), Unsharp Masking filter (Gaussian kernel  $7 \times 7$ ), Savitzky-Golay 2nd derivative filter ( $M = 4$ ,  $m = 9$ )

### 3.2.2 Object measurement in Astrometry

The adjusted images were saved and opened in *Astrometry* software for carrying out the astrometric measurements. Using the same parameters settings (BoxSize 5, SNR for Display/Reduction 2.5, SNR for Identification 6.0), images were reduced to detected objects and displayed.

The reduction of original image to objects, along with the reduction of the images processed by the suggested methods, are displayed in the Figure 2. Since only four of the six methods were able to provide enhancement of the image, only these four are depicted. The yellow dots represent objects which will enter identification algorithm, the gray dots represent the rest of the detected objects. The red dots stand for overexposed objects and the blue dots for diffuse objects.

Let us compare the first three methods, which employ a set of images for background flattening. They all offer drastically better object detection than the unprocessed image, as well as enhancing their SNR and, consequently, positional accuracy. **Kappa-sigma clipping flatfield** seems to perform slightly better than **Median flatfield**, and **SMIN flatfield** performs slightly worse. Choosing a very faint object at random, it shows its SNR is undetectable at the raw image ( $\text{SNR} < 0.7$  results in range check error due to too many possible objects), while with median filter its SNR is 4.9, with kappa-sigma clipping flatfield it is 5.3 and with SMIN flatfield 4.4.

Let's inspect astrometric performance of  **$\alpha$ -quantile flatfield**, which requires only single image.  $\alpha$ -quantile flatfield with  $\alpha=0.5$ ,  $m = 13$  offers a very even result across the whole field of view, as seen in Figure 2, although not as good as previous methods, which can be attributed to the fact we are dealing only with one image instead of a whole set. The same faint object as before now has SNR 3.5.

Now for the last two methods, which are not included in Figure 2. **Unsharp masking filter** enhanced contrast of the noise, making *Astrometry* run into 'Range check error' already at 1.2 SNR, and the chosen faint object is impossible to measure on the image. **Savitzky-Golay filter**'s 2nd derivative is out of question due to inability to discern faint objects altogether.

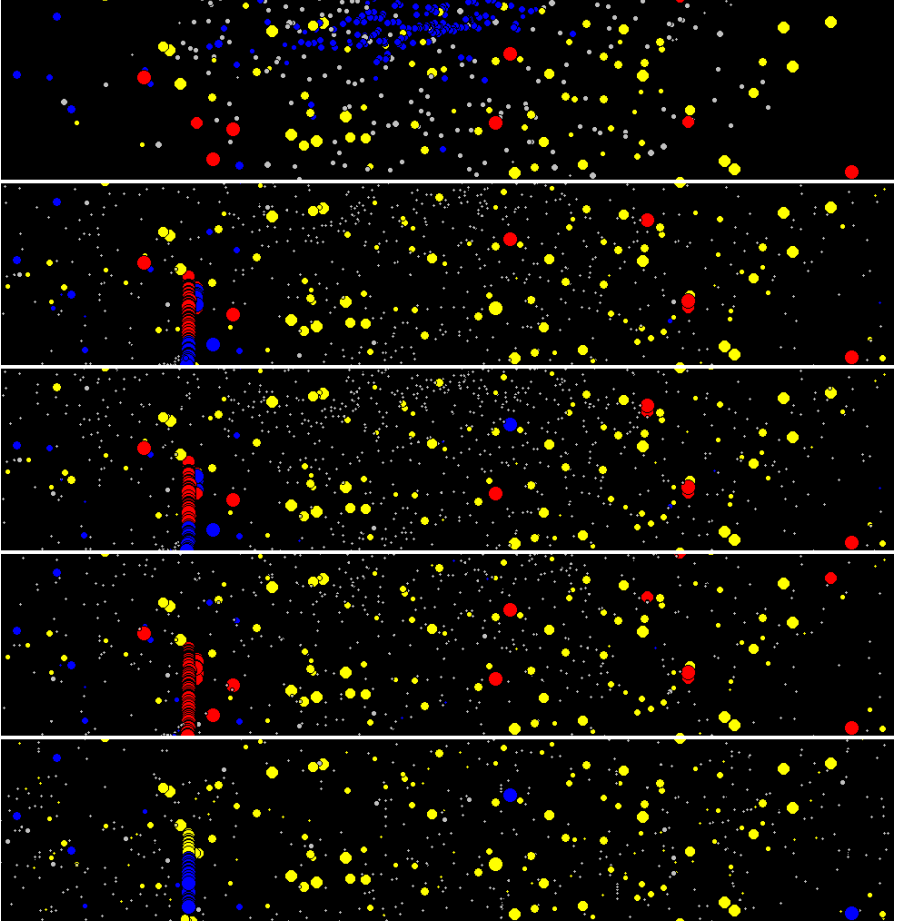


Figure 2: Comparison of images' astrometry. Image cut-outs from top to bottom: Raw image, Median flatfield, Kappa-sigma clipping flatfield, SMIN flatfield,  $\alpha$ -quantile flatfield ( $\alpha = 0.5$ ,  $m = 13$ ).

### 3.3 Recommendations for use

The use of these methods newly programmed into *Blink* is discussed in this section to serve as guidance for the observers using the program. Four of the tested methods mean a huge leap in quality — or even possibility — of the astrometric measurement for KLENOT project, although there are conditions which make one or another more useful.

For an image set where the stellar field shifts slightly between the images, it is recommended to use my customized **kappa-sigma clipping flatfield** to create an artificial flatfield for the set. In the case when the stellar 'shadows' are too pronounced while using this method, it is advised to use **SMIN flatfield** instead.

For a single image or stars moving too slowly across the field of view, it is recommended to use the newly devised  **$\alpha$ -quantile flatfield** with default  $\alpha = 0.5$ ,  $m = 13$  for creation of artificial flatfield. Its superior advantage is the ability to generate artificial flatfield from a single image.

The rest of the examined methods are not suitable for our use in astrometry of faint asteroids. **Median flatfield** is replaced by better kappa-sigma clipping flatfield, and neither **unsharp masking filter** or 2nd derivative of **Savitzky-Golay filter** were able to provide utilizable results.

*Blink* also provides an option to save the modified images, which are then in turn loaded into *Astrometry* to carry out the astrometric measurement itself.

## 4 First results: Interstellar body 1I/2017 U1 'Oumuamua

The small object with extreme speed was discovered on 19th October 2017 by Pan-STARRS and originally designated as comet C/2017 U1 due to its atypical orbit. No cometary features were detected and the designation was changed to inactive comet A/2017 U1. Excentricity of its orbit was  $e = 1.18$ , which corresponds to hyperbolic orbit, placing the origin of the object outside the Solar System. The object's designation was changed again and 1I/2017 U1, named 'Oumuamua — meaning 'Scout' in Hawaiian, became the first member of newly created category of Interstellar objects.

The body is elongated, with size estimated to be about 230 by 35 meters, and composed of metal-rich rock, with dark red hue at the surface associated with longterm exposition to cosmic radiation. It flew past the Sun and left the Solar System in the direction of Pegasus constellation.

1.06-m KLENOT telescope observed the object on 19th October 2017, when ten 5-second exposures were taken. The experienced measurer M. Tichý was unable to process the images of the fast, faint body for astrometric positions, as it was 20.4 mag (V band) in the time of observation.

The images were treated with SMIN method the author of this work programmed into *Blink*. It was then possible to measure the object's position in *Astrometry*. The astrometric measurements were published in [4] together with the object's astrometry from 2.4-m telescope in New Mexico, USA, and 5.0-m telescope on Mt. Palomar, USA.

## 5 Conclusion

The short version of the doctoral thesis *Numerical Methods of Image Analysis in Astrometry* gives an introduction to astrometric measurement of small Solar System bodies. The aim of the thesis is 'to find a suitable mathematical method to even out the background of a CCD image without affecting the small irregularities containing combined noise and data to achieve increase in both quality and quantity of astrometric measurements on Klet Observatory'[5].

Total six promising methods were chosen to be programmed into *Blink*, software for image processing and viewing in routine use by Klet Observatory, which the author of this work is developing. Four from the six methods were successful in evening out the background of the CCD images without tampering with its high frequency components. Median flatfield and Kappa-sigma clipping flatfield make use of the stellar field's drift between images of the set, while SMIN flatfield can be applied even on static set.  $\alpha$ -quantile flatfield requires only single image to perform its task. These methods allow for astrometric measurements to be carried out even in unfavorable conditions, e.g. at areas where the raw image was darker or brighter than the average background for the image, or pronounced background intensity gradient was present, where astrometry would be impossible before. Additionally, flattening the background by these methods raises the SNR of the objects, thus it is recommended to apply these methods even in the cases when the astrometry can be performed on the raw images, to raise the precision of the result. Not only these methods can be applied on new observations, but they can be also utilized on an extensive archive of CCD images for precovery use.[3]

The new image processing routines were immediately used and allowed astrometry of the first, and so far the only known, interstellar object 1I/2017 U1 ('Oumuamua)[4].

The doctoral thesis fulfills the goals set in the treatise as written above.

# Bibliography

## Author's publications

- [1] TICHÁ, J., TICHÝ, M., KOČER, M., HONKOVÁ, M., KLENOT PROJECT 2002–2008 contribution to NEO astrometric follow-up, *Meteorit. Planet. Sci.*, 2009, vol. 44, Issue 12, pp. 1889–1895. doi: 10.1111/j.1945-5100.2009.tb01998.x
- [2] TICHÝ, M., HONKOVÁ, M., TICHÁ, J., KOČER, M., *Inaccuracies Affecting the Calculation of Orbital Elements*, presented at 2013 IAA Planetary Defense Conference, Flagstaff, AZ, USA, 2013. (submitted to Experimental Astronomy).
- [3] TICHÝ, M., TICHÁ, J., KOČER, M., HONKOVÁ, M., *TNO Preccovery Survey Using the KLENOT Telescope Archive*, presented at Asteroids, Comets, Meteors 2008 held July 14–18, 2008 in Baltimore, Maryland, USA. LPI Contribution No. 1405, paper id. 8067. Bibliographic Code: 2008LPICo1405.8067T
- [4] TICHÝ, M., TICHÁ, J., HONKOVÁ, M., BLAGORODNOVA, N., YE, Q.Z., ZHANG, Q., PEFFER, K., RYAN, W.H., RYAN, E.V., WILLIAMS, G.V., *A/2017 U1*, Minor Planet Electronic Circ., No. 2017-U265, 2017. Available from <https://minorplanetcenter.net/mpec/K17/K17UQ5.html>
- [5] HONKOVÁ, M., *Numerical Methods of Image Analysis in Astrometry*, Doctoral thesis statement, Faculty of Mechanical Engineering, Brno University of Technology, 2014.
- [6] HONKOVÁ, M., *Následná astrometrie blízkozemních planetek a její vliv na přesnost určení dráhových elementů a efemerid*, Bachelor's thesis, Faculty of Science, Masaryk University, Brno, 2006. Available from [https://is.muni.cz/th/106774/prif\\_b/Nasledna\\_Astrometrie\\_-\\_Honkova.pdf](https://is.muni.cz/th/106774/prif_b/Nasledna_Astrometrie_-_Honkova.pdf)

## Other references

- [7] GUEST, P.G., *Ch. 7: Estimation of Polynomial Coefficients. Numerical Methods of Curve Fitting*. Cambridge University Press, 1961, re-edition in 2012. pp. 147—. ISBN 978-1-107-64695-7.
- [8] HAMMING, D.F., *Digital Filters*. 2nd. ed., (Englewood Cliffs, NJ: Prentice Hall), 1983.

- [9] PRESS, W.H., TEUKOLSKY, S.A., VETTERLING, W.T., FLANNERY, B.P., *Numerical Recipes in C: The Art of Scientific Computing* 2nd ed., Cambridge University Press, ISBN 0-521-43108-5.
- [10] SAVITZKY, A., GOLAY, M.J.E., Smoothing and Differentiation of Data by Simplified Least Squares Procedures. *Analytical Chemistry*. 36 (8): 1627—39. 1964. doi: 10.1021/ac60214a047.
- [11] STEINIER, J., TERMONIA, Y., and DELTOUR, J., Comments on Smoothing and Differentiation of Data by Simplified Least Square Procedure. *Analytical Chemistry*. 44 (1972), pp. 1906–1909. Available at: <https://www.people.iup.edu/jford/courses/CHEM421/Resources/CommentsOnSmoothingAndDifferentiationOfDataBySimplifiedLeastSquareProcedure.pdf>
- [12] SHEKHAR, C., On Simplified Application of Multidimensional Savitzky–Golay Filters and Differentiators, *Progress in Applied Mathematics in Science and Engineering*, 2015, Bali, Indonesia. doi: 10.1063/1.4940262
- [13] NIKITAS, P., PAPPA-LUISI, A., Comments on the two-dimensional smoothing of data. *Analytica Chimica Acta*. 415: 117–125, 2000. doi: 10.1016/S0003-2670(00)00861-8
- [14] ZIEGLER, H., Properties of Digital Smoothing Polynomial (DISPO) Filters. *Applied Spectroscopy*, vol. 35, pp. 88–92, 1981. doi: 10.1366/0003702814731798
- [15] *U.S. Naval Observatory (USNO)*,  
<http://www.usno.navy.mil/USNO/astrometry/optical-IR-prod>



# Curriculum Vitae

**Name:** Michaela Honková  
**Address:** Čechova 54, České Budějovice, 37004, Czech Republic  
**Contact:** tel. (+420) 775 398 984, e-mail honkova84@gmail.com

## Education

from 2011 **Ph.D. student of Applied Mathematics** at Institute of Mathematics, Faculty of Mechanical Engineering, **Brno University of Technology**  
2003-2008 **Master's degree (Mgr.) and bachelor degree (Bc.)** in Theoretical physics and astrophysics at Faculty of Science, **Masaryk University** in Brno

## Work experience

from 2017 **contracted programmer** for Klet Observatory for systemic development and upkeep of special software and databases  
2008-2017 **research staff** at Klet Observatory, branch of Observatory and planetarium České Budějovice (HaP), member of KLENOT team; study, analysis and solving of research and developmental tasks regarding astrophysics; operator of a telescope, independently carrying out astrometric measurements of asteroids and comets; development of custom software for Klet Observatory; attending international conferences including paper and poster preparation and presentation.  
2007-2017 **educational staff** at HaP, lecturing special programs, creation of multimedia and tools, carrying out observations of asteroids and comets and their astrometry  
2006-2017 **lecturer** for public at HaP, telescope operator

## Knowledge and skills

<b>Languages</b>	native Czech, fluent English
<b>Computer skills</b>	<b>Delphi</b> programming language (Object Pascal) L <sup>A</sup> T <sub>E</sub> X typographic system, MySQL databases, Adobe Flash, MS Office, Windows.
<b>Other Skills</b>	<b>driver's licence</b> group B

## **Abstrakt**

Velmi přesná následná astrometrie je nezbytným předpokladem sledování blízkozemních objektů, které mohou představovat riziko srážky se Zemí. Tato práce přináší ucelený přehled přesné astrometrie, obsahuje potřebnou matematickou teorii, postup předzpracování snímků v astronomii, a nastiňuje použití filtrů. Navrhuje nové metody pro vyrovnání pozadí snímků před provedením astrometrického měření pro případ, kdy nejsou dostupné kalibrační snímky. Tyto metody jsou založeny na vytvoření syntetického flatfieldu pomocí aplikování filtru na snímek a následné užití tohoto flatfieldu pro odstranění pozadí snímku. Metody byly otestovány na vzorových snímcích a vzápětí použity k získání astrometrických pozic prvního mezihvězdného objektu 1I/2017 U1 ('Oumuamua).

## **Abstract**

High-precision follow-up astrometry is essential for tracking Near-Earth Objects, which may pose risk of impact to the Earth. This thesis brings an overview of astrometric process and requirements of precise astrometry, contains the necessary mathematical background, steps of image pre-processing in astronomy, and outlines the use of filters. New methods are proposed to level the background of images prior to performing astrometric measurements for cases when no calibration images were taken. They are based around applying filters on an image to create artificial flatfield, which is then applied back on the image. These methods are tested on sample data and immediately used to obtain astrometry of the first interstellar object 1I/2017 U1 ('Oumuamua).